Behaviour of Headed Anchor Blind Bolts Embedded in Concrete Filled Circular Hollow Section Column

Yusak Oktavianus[1], Helen M. Goldsworthy[2], Emad F. Gad[3]

1. Corresponding Author. PhD Candidate, Department of Infrastructure Engineering, The University of Melbourne, Parkville, Victoria 3010.
   Email: yoktavianus@student.unimelb.edu.au

2. Associate Professor, Department of Infrastructure Engineering, The University of Melbourne, Parkville, Victoria 3010.
   Email: helenmg@unimelb.edu.au

3. Professor, Faculty of Science, Engineering & Technology, Swinburne University of Technology, Hawthorn, Victoria 3122.
   Email: egad@swin.edu.au

Abstract

Blind bolts allow technicians to connect the steel beam and Concrete Filled Circular Hollow Sections (CFCHS) column from the outside of CHS. In addition, using blind bolts as the connection may avoid the brittle behaviour generated by the welded connections. However, there are currently no guidelines and clear understanding of the behaviour of this connection. This paper presents the results of finite element studies on pull-out behaviour of various dimensions of groups of headed anchor blind bolts (HABBs) embedded in CFCHS with various *D/t* ratios in both 90° and 180° T-stub. Several parameters, such as θ value, additional blind bolt in shear, additional through bolt, *D/t* ratio, and embedment depth, were investigated to gain a better understanding of the behaviour of this connection.

Keywords: pull out, blind bolt, headed anchor blind bolt, concrete filled circular hollow section

1. Introduction

Concrete Filled Circular Hollow Sections (CFCHS) have a pronounced advantage relative to steel columns in terms of structural strength and stiffness, and aesthetic appearance. Also, they are inherently ductile because of the high level of confinement of concrete provided by the steel tube and are hence favoured for use in moment-resisting frames in areas of high seismicity such as Japan. Learning from the 1994 Northridge earthquake, a lot of brittle fractures were initiated at complete joint penetration (CJP) weld between the bottom flange of the beam and column flange at very low levels of plastic demand (FEMA-351, 2000). A summary of the typical failure modes in the welded joint is presented by Tremblay et al. (1995). Moreover, the lack of access to the inside of circular hollow sections challenges the wider use of this section in the industry.

The use of a new type of bolts in which the nut can be tightened from only one side (so called "blind bolts") should overcome the two problems discussed above. Blind bolts allow technicians to connect the steel beam and Concrete Filled Circular Hollow Sections (CFCHS) column from the outside of CHS; also using blind bolts to connect T-stubs to the CFCHS

column may avoid the brittle behaviour generated by the welded connections. There are several blind bolts that are available in the market. Those are the Huck high-strength blind bolt (Huck International Inc., 1990), the Lindapter Hollo-bolt (Lindapter International Ltd., 1995), Flow-drilling (France et al., 1999a), and the AJAX ONESIDE blind bolt (AJAX Engineered Fasteners, 2002). AJAX ONESIDE blind bolts have been chosen and will be utilized in this paper to describe the mechanical behaviour of the blind bolts embedded in CFCHS.

A feasibility study for cogged anchor blind bolt (CABB) connections to CFCHS was carried out by Goldsworthy & Gardner (2006). Yao et al. (2008; 2011) used single and groups of cogged anchor blind bolts (CABBs) and single headed anchor blind bolts (HABBs) in CFCHS. Specimens with *D/t* ratio from 32.4 to 54 were used in pull-out tests of single HABBs in CFCHS. Since there are currently no guidelines and clear understanding of the behaviour of this connection, this paper presents finite element studies on pull out tests of various dimensions of groups of headed anchor blind bolts (HABBs) embedded in CFCHS with various *D/t* ratios and in both 90° and 180° T-stubs. The *D/t* ratios are chosen on the basis that local buckling should be prevented. AISC (2010) limits the *D/t* ratio for compression steel elements in composite members subject to axial compression ($0.15E/f_y$) and flexure ($0.09E/f_y$). Both of those limitations are for compact sections. Hence, if 350L0 steel tubes are used, the maximum *D/t* ratio that can be used is approximately equal to 51. Therefore, *D/t* ratios between 30 to 51 will be used in this paper. The endplate of the curved T-stub used in this study has been designed to have a thickness of 25 mm so that it will remain elastic. Several parameters, such as θ value, additional blind bolt in shear, additional through bolt (TB), *D/t* ratio, and embedment depth, were investigated to gain a better understanding of the behaviour of this connection.

2. Details of the specimens

Details of the specimens are shown in Table 1 and Figure 1. BB and TB represent ordinary blind bolts (without extensions) and through bolt, respectively.

Table 1. Details of the specimens

Specimen	Tube size	*D/t*	Top of curved T-stub	Bottom of curved T-stub	degree of T-stub (°)	Note
H90-1	CHS 457x9.5	48.1	1M20 HABB	1M20 HABB	90	group of HABB
H90-2	CHS 457x9.5	48.1	2M20 HABB	2M20 HABB	90	group of HABB
H90-3	CHS 457x9.5	48.1	2M24 HABB	2M24 HABB	90	group of HABB
H180	CHS 457x9.5	48.1	4M24 HABB	4M24 HABB	180	group of HABB
HB180	CHS 457x9.5	48.1	2M24 HABB + 2M24 BB	2M24 HABB + 2M24 BB	180	group of HABB and BB
HT90-1	CHS 457x9.5	48.1	2M20 HABB + 1M24 TB	2M24 HABB	90	group of HABB and TB
HT90-2	CHS 457x9.5	48.1	2M20 HABB + 1M24 TB	2M24 HABB_120mm	90	group of HABB and TB
HT90-3	CHS 457x12.7	36	2M20 HABB + 1M24 TB	2M24 HABB	90	group of HABB and TB
HT90-4	CHS 457x9.5	48.1	2M24 HABB + 1M30 TB	2M30 HABB	90	group of HABB and TB

All of the HABBs have effective embedment depth, h_{eff}, of 100 mm plus the thickness of the washer, except the HABB in the bottom of curved T-stub in specimen HT90-2 which has h_{eff} equal to 120 mm plus the thickness of the washer. The thicknesses of the washer for M20, M24 and M30 are 6 mm, 7 mm and 8.5 mm, respectively.

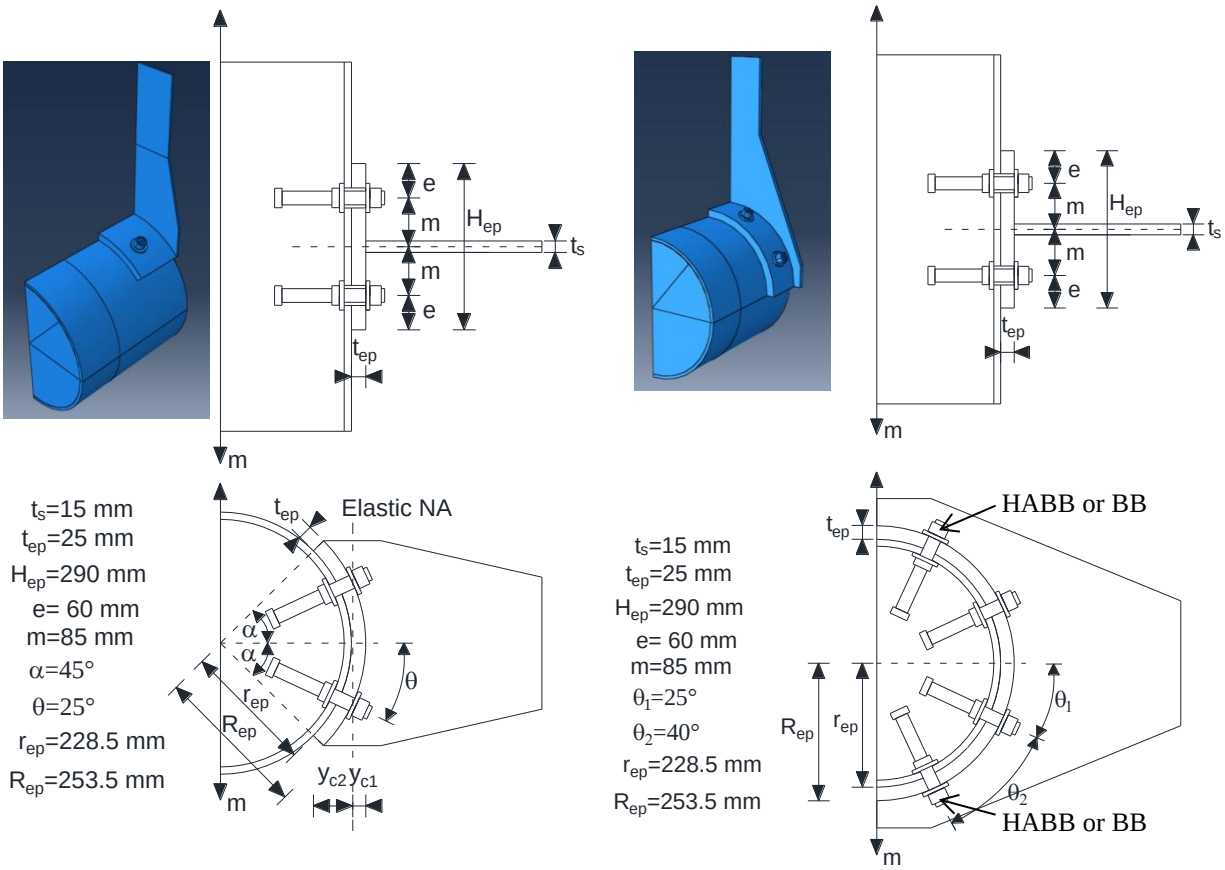

(a) 90° T-stub (H90-2 and H90-3) (b) 180° T-stub (H180 and HB180)

Figure 1. Configuration of the specimen and the FEA modelling

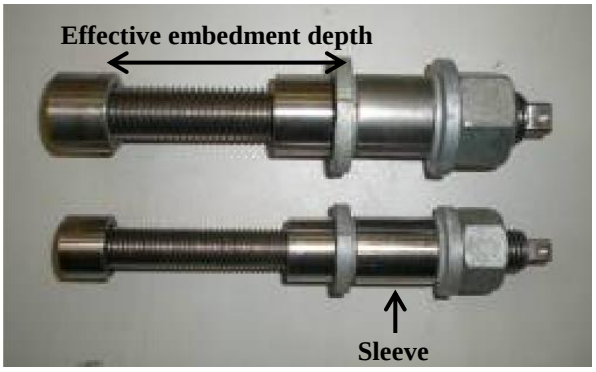

Figure 2. Headed anchor blind bolt (HABB)

3. Finite element (FE) modelling

ABAQUS (2012) was used for executing the finite element analyses. Figure 1 shows the quarter model for the FE modelling of specimens H90-2, H90-3, H180, and HB180. A displacement boundary condition was applied at the tip of the T-stub stem to represent the pull-out action from the hydraulic jack. The bolt and nut were modelled as one solid element.

The collapsible washer was also modelled as a solid washer. Minimum pretension force was applied using temperature pressure to the middle of the shank of the blind bolt to clamp the curved T-stub flange and steel tube together. The coefficient of friction used between the concrete and the HABB is equal to 0.3 as recommended by Guezouli and Lachal (2012), whereas the coefficient of friction used between steel and steel is assumed to be equal to 0.3. Nominal material properties were used for steel elements as shown in Table 2, where $f_y, f_p,$ and f_u represent yield stress for steel, proof stress for bolt, and ultimate strength, respectively. A concrete compressive strength of 48 MPa was used. Concrete damage plasticity was chosen for representing the concrete plastic behaviour. The fracture energy stated in the ABAQUS documentation (ABAQUS, 2012) was used for modelling the concrete behaviour in tension. Fracture energy which is equal to 150 N/m was used for the concrete strength of 48 MPa. The tensile strength of the concrete was assumed to be equal to $0.56\sqrt{f_c'}$ (ACI 318M, 2011).

Table 2. Material properties for steel tube, T-stub, blind bolt, nut, and washer

Note	Steel tube	Curved T-stub		Blind bolt, nut, and washer
		Endplate	Flared flange	
f_y *or* f_p (MPa)	350	280	310	600
f_u (MPa)	430	410	430	830

4. Finite element analysis (FEA) results and discussion

The results from FEA were separated into different sub-sections to understand the effect of different parameters to the pull-out force vs displacement relationship. The parameters are θ value, additional blind bolt in shear, additional through bolt, *D/t* ratio, and embedment depth.

4.1. Effect of inclination

Specimens with 90° curved T-stubs, H90-1 and H90-2 in particular, were compared. Specimen H90-1 which has 2M20 blind bolts needed to be multiplied by 2 to be compatible with H90-2 which has 4M20 blind bolts. The difference is that H90-1 has no θ value, whereas H90-2 has θ value equal to 25° (see Figure 1 for clear presentation of θ). Figure 3 gives a plot of the force vs displacement from the FEA. The force represents the pull-out force applied to the tip of the curved T-stub, whereas the displacement represents the outward displacement at the middle of blind bolt's head (Figure 3(b)) and the outward displacement at the middle of the curved endplate of T-stub (Figure 3(a) and other Figures). Figure 3 shows that both 2x H90-1 and H90-2 will produce similar ultimate strengths. However, the value of ultimate strength of H90-2 is 2% less than the ultimate tensile capacity of 4M20 blind bolts. Figure 4 also shows that the ultimate strength of HB180 with 4 HABBs at $\theta = 25°$ and 4 HABBs at $\theta = 65°$ is less than the ultimate tensile strength of 8M20 blind bolts. This is because in the case of H90-2 (θ equal to 25°) and H180 (θ equal to 25° and 65°), the pull-out force from the T-stub will be distributed as tensile and shear forces to the bolt, and the bolt will fail in combined shear and tension instead of in pure tension. Table 3 gives the capacity reduction ratio for blind bolts at different value of θ. These have been derived using Eq. (1) below from AS 4100 (AS 4100, 1998).

$$\left(\frac{V_f^*}{\emptyset V_f}\right)^2 + \left(\frac{N_{tf}^*}{\emptyset N_{tf}}\right)^2 \leq 1.0 \quad (1)$$

$$V_f^* \leq \emptyset V_f = 1 \cdot 0.62 \cdot k_r \cdot f_{uf} \cdot (n_n A_c + n_x A_o) \quad (2)$$

$$N_{tf}^{*} \leq \emptyset N_{tf} = 1 \cdot A_s \cdot f_{uf} \quad (3)$$

Using several assumption as follows: $\emptyset = 1$; thread area excluded when calculating the shear area; and using M20 grade 8.8 as an example, Table 3 shows that the pull-out capacity is expected to reduce as the θ value is increased. AS4100 provided more conservative result compared with FEA at $\theta = 25°$. Using a capacity reduction factor equal to 0.95 for blind bolts at $\theta = 25°$, the capacity reduction factor for blind bolts at $\theta = 65°$ in HB180 was calculated using FEA and it resulted the same value as obtained in AS4100.

Table 3. Pull-out capacity at different value of θ

θ (°)	Pull-out capacity (kN)	V_f^* (kN)	N_{tf}^* (kN)	combination ratio	$\frac{\text{pull}-\text{out capacity}}{\text{pull}-\text{out capacity at } \theta = 0}$	
					AS4100	FEA result
0	203.35	0.00	203.35	1.00	1.00	1.00
25	193.55	81.80	175.42	1.00	0.95	0.975 (H90-2)
65	189.96	94.98	164.51	1.00	0.82	0.82 (HB180)

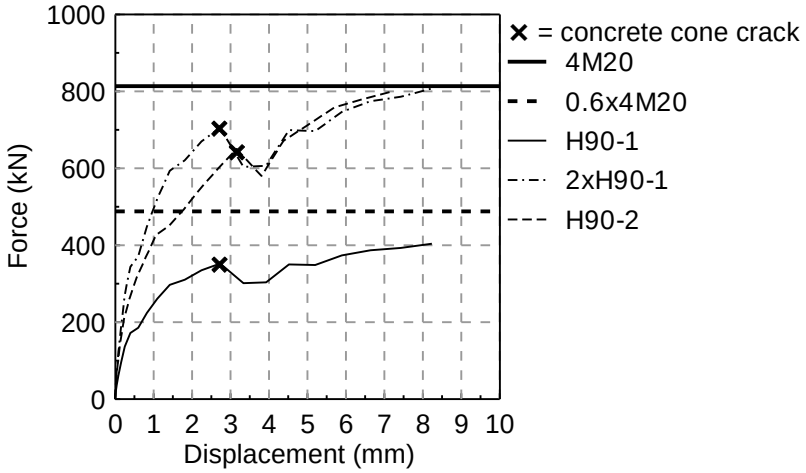

(a) Including the effect of elastic curved T-stub

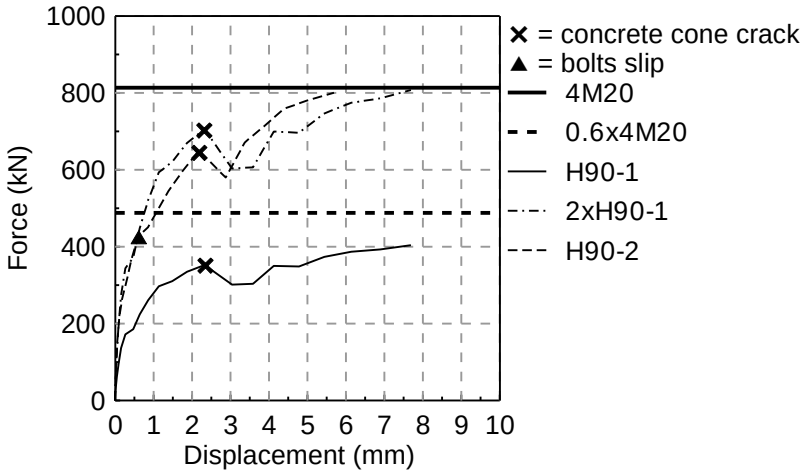

(b) Without the effect of elastic curved T-stub

Figure 3. Effect of inclination

With regards to the effect of the angle of inclination, θ, on the stiffness, comparison have been made between specimen 2x H90-1 and H90-2, and between 2x H90-3 and H180. With the elastic deformation of the curved T-stub included in the determination of deformation (Figure 3(a)), the secant stiffness at 60% of ultimate capacity was reduced from 519 kN/mm to 340 kN/mm (decreased about 35%). In Figure 4, the secant stiffness at 60% of ultimate capacity of 2x H90-3 also decreased about 35% compare with that of H180.

Figure 3(b) shows clearly when the slip occurred in the case of H90-2. The slip force, S_f, can be calculated as follows:

$$S_f = \frac{n \cdot \mu_s \cdot F_p}{\sin\theta} \tag{4}$$

where n is the number of blind bolts that have same θ value, F_p is the pretensioned force applied to the blind bolts (approximately equal to 70% of ultimate capacity of the blind bolt); μ_s is static coefficient of friction (assumed to be equal to 0.3). In the case of H90-2, $S_f = \frac{4 \cdot 0.3 \cdot 145}{\sin 25°} = 412$ kN. This value is similar to the value obtained in FEA which is equal to 426 kN.

4.2. Effect of additional blind bolt in shear

The specimen with a 90° curved T-stub (H90-3) was compared with specimens with a 180° curved T-stub (H180 and HB180) to comprehend the effect of the additional HABBs or BBs in shear. As shown in Figure 4, additional HABBs or BBs in shear increased the ultimate capacity by less than twofold. This is because the effect of the inclination that has been explained above. For the stiffness at 60% of ultimate capacity, the stiffness of H180 and HB180 was about 31% and 21% larger than that of H90-3. Hence, HABBs in shear in H180 were not very effective in increasing the stiffness, and there was only a small increase in stiffness induced by using headed anchor blind bolts (HABBs) rather than ones without anchors (BBs)

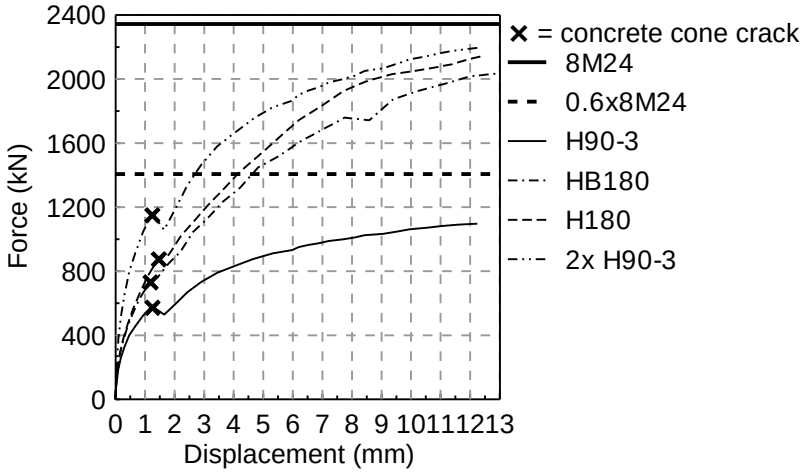

Figure 4. Effect of HABBs or BBs in shear

4.3. Effect of additional through bolt (TB)

Figure 5 shows that though the ultimate strength of H180 is much larger than that of HT90-4, the secant stiffness at 60% of ultimate capacity of H180 is lower than that of HT90-4. This means an additional through bolt will be more effective than 4 additional HABBs in shear in increasing the stiffness. The TB will prevent the bolts in the same elevation of the TB from slipping. Using the value given in Table 3, the contribution of the TB was calculated. It was shown that only 86% capacity of the TB is able to be added to the system since the ultimate tensile capacity of the groups of HABBs at the bottom of the T-stub was reached at this stage.

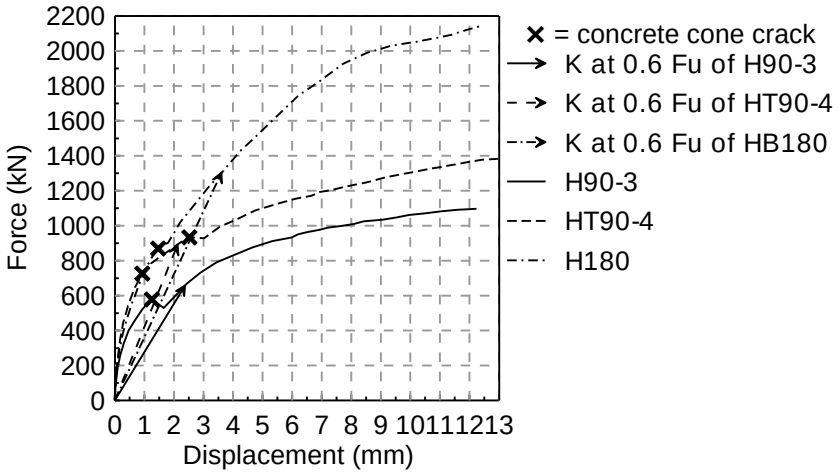

Figure 5. Effect of through bolt

4.4. Effect of *D/t* ratio and embedment depth

Concrete cones formed by the bearing of the headed anchor on the concrete could overlap horizontally, vertically, or both. In general, the overlap between the cones occurred horizontally prior to occurring vertically. This is simply because of the smaller distance between the heads of the adjacent HABBs in the horizontal direction than in the vertical direction. Figure 6 presents the effect of increasing the embedment depth and decreasing the *D/t* ratio. As the effective embedment depth of HABBs at the bottom of the curved T-stub was increased from 107 mm in the case HT90-1 to 127 mm in the case of HT90-2, both stiffness and strength increased and the concrete cone was delayed until 0.7 of the ultimate capacity of (3M24+2M20). This means that in the case of D=457 mm and t=9.5 mm (D/t = 48.1), effective embedment depth approximately equal to 5 times the diameter of the blind bolt should be provided to ensure that the concrete has sufficient cone area to take the pull-out force transferred by the HABBs. The strength and stiffness increased as the *D/t* ratio was reduced from 48.1 in the case HT90-1 to 36 in the case of HT90-3. The increased participation of bearing of the washer on the steel tube wall helped to delay the formation of the cone in this case.

Increasing the diameter of the blind bolt without increasing the embedment depth or reducing the *D/t* ratio will not effectively increase the stiffness and the capacity of the system (compare case HT90-4 with HT90-1). The ultimate capacity of HT90-4 was only about 75% of ultimate capacity of 2M24+3M30 and concrete cone developed early (below 0.6x(2M24+3M30)).

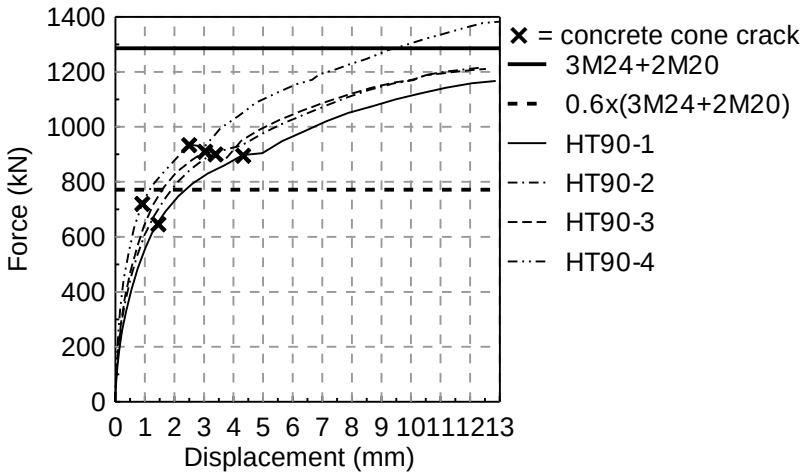

Figure 6. Effect of embedment depth and *D/t* ratio

5. Conclusions

Extensive finite element analyses (FEA) on the group behaviour of headed anchor blind bolts (HABBs) embedded in concrete filled circular hollow section (CFCHS) columns were accomplished. Several parameters, such as θ value, additional blind bolt in shear, additional through bolt, *D/t* ratio, and embedment depth, were investigated to gain a better understanding of the behaviour of this connection. The HABBs were pretensioned to ensure that the curved T-stub was well clamped to the CHS. Curved T-stub was designed to remain in the elastic range of the material behaviour. Several conclusions were made and can be summarised as follows:

1. Pull-out capacity of the connection decreased as the θ value increased. This is because there is a combined force in shear and tension. Reduction of the pull-out capacity of the connection can be calculated by maintaining the combination ratio to be equal to 1. Moreover, reduction in stiffness by 35% each time should be considered as θ changed from 0° to 25° and from 25° to 65° when the elastic deformation of the curved endplate of T-stub is taken into account.
2. HABBs in shear provided similar stiffness compared with BBs in shear. This is because the shear is dominating and hence the headed anchor will not contribute much in increasing both the stiffness and strength.
3. It was shown that only 86% capacity of the TB can be added to the system and it depended on the total ultimate tensile capacity of the groups of HABBs in the bottom of the T-stub (which is always lower than that of in the top). It was also shown that the secant stiffness at 60% of ultimate capacity of the system using TB is larger than that of the system using 4 additional BBs in shear.
4. As the effective embedment depth of HABBs at the bottom of the curved T-stub was increased from 107 mm in the case HT90-1 to 127 mm (roughly equal to 5xHABB diameter) in the case of HT90-2, both the stiffness and strength increased and the concrete cone was delayed until 0.7 of the ultimate capacity of (3M24+2M20).
5. The strength and stiffness also increased as the *D/t* ratio was reduced from 48.1 in the case of HT90-1 to 36 in the case of HT90-3. Increasing the diameter of the blind bolt without increasing the embedment depth or reducing the *D/t* ratio will not effectively increase the stiffness and the capacity of the system.

References

ABAQUS. (2012). ABAQUS 6.12 documentation. Providence, USA: Dassault Systèmes Simulia Corp.

ACI 318M. (2011). Building code requirements for structural concrete (ACI 318M-11) and commentary. USA: American Concrete Institute.

AISC. (2010). Specification for Structural Steel Buildings. United States of America: American Institute of Steel Construction.

AJAX Engineered Fasteners. (2002). ONESIDE brochure. B-N012 data sheet. Victoria, Australia.

AS 4100. (1998). Australian Standard: Steel Structures. Sydney, Australia: Standards Australia Limited.

FEMA-351. (2000) Recommended seismic evaluation and upgrade criteria for existing welded steel moment-frame buildings (pp. 2-9).

France, J. E. Davison, J. B. and Kirby, P. A. (1999a) Strength and rotational stiffness of simple connections to tubular columns using flowdrill connectors. Journal of Constructional Steel Research Vol 50, pp 15-34.

Goldsworthy, H. M. and Gardner, A. P. (2006) Feasibility study for blind-bolted connections to concrete-filled circular steel tubular columns. Structural Engineering and Mechanics Vol 24, pp 463-478.

Guezouli, S. and Lachal, A. (2012) Numerical analysis of frictional contact effects in push-out tests. Engineering Structures Vol 40, pp 39-50.

Huck International Inc. (1990). Industrial fastening systems. Arizona, USA.

Lindapter International Ltd. (1995). Type HB hollo-bolt for blind connection to structural steel and structural tubes. Bradford, England.

Tremblay, R. Timler, P. Bruneau, M. and Filiatrault, A. (1995) Performance of steel structures during the 1994 Northridge earthquake. Canadian Journal of Civil Engineering Vol 22, pp 338-360.

Yao, H. Goldsworthy, H. M. and Gad, E. F. (2008) Experimental and Numerical investigation of the tensile behaviour of blind-bolted T-stub connections to concrete-filled circular column. Journal of Structural Engineering, American Society of Civil Engineers Vol 134, pp 198-208.

Yao, H. Goldsworthy, H. M. Gad, E. F. and Fernando, S. (2011) Experimental Study on Modified Blind Bolts Anchored in Concrete-Filled Steel Tubular Columns, Australian Earthquake Engineering Society Conference, Novotel Barossa Valley Resort, South Australia.